**Applied Physics A manuscript No.**
(will be inserted by the editor)



# Ferromagnetic 0–$\pi$ Josephson junctions

**M. Weides[1], H. Kohlstedt[1], R. Waser[1], M. Kemmler[2], J. Pfeiffer[2], D. Koelle[2], R. Kleiner[2], E. Goldobin[2]**

[1] Center of Nanoelectronic Systems for Information Technology (CNI), Research Centre Jülich, D-52425 Jülich, Germany
[2] Physikalisches Institut-Experimentalphysik II, Universität Tübingen, Auf der Morgenstelle 14, D-72076 Tübingen, Germany

Received: date / Revised version: date

**Abstract** We present a study on low-$T_c$ superconductor-insulator-ferromagnet-superconductor (SIFS) Josephson junctions. SIFS junctions have gained considerable interest in recent years because they show a number of interesting properties for future classical and quantum computing devices. We optimized the fabrication process of these junctions to achieve a homogeneous current transport, ending up with high-quality samples. Depending on the thickness of the ferromagnetic layer and on temperature, the SIFS junctions are in the ground state with a phase drop either 0 or $\pi$. By using a ferromagnetic layer with variable step-like thickness along the junction, we obtained a so-called 0-$\pi$ Josephson junction, in which 0 and $\pi$ ground states compete with each other. At a certain temperature the 0 and $\pi$ parts of the junction are perfectly symmetric, i.e. the absolute critical current densities are equal. In this case the degenerate ground state corresponds to a vortex of supercurrent circulating clock- or counterclockwise and creating a magnetic flux which carries a fraction of the magnetic flux quantum $\Phi_0$.

## 1 Introduction

Superconductivity (S) and ferromagnetism (F) are two competing phenomena. On one hand a bulk superconductor expels the magnetic field (Meissner effect). On the other hand the magnetic field for $H > H_{c2}$ destroys the superconductivity. This fact is due to the unequal symmetry in time: ferromagnetic order breaks the time-reversal symmetry, whereas conventional superconductivity relies on the pairing of time-reversed states. It turns out that the combination of both, superconductor and ferromagnet, leads to rich and interesting physics. One particular example – the phase oscillations of the superconducting Ginzburg-Landau order parameter inside the ferromagnet – will play a major role for the devices discussed in this work.

The current-phase relation $I_s(\phi)$ of a conventional SIS Josephson junction (JJ) is given by $I_s(\phi) = I_c \sin(\phi)$. $\phi = \theta_1 - \theta_2$ is the phase difference of the macroscopic superconducting wave functions $\Psi_{1,2} = \sqrt{n_s} e^{i\theta_{1,2}}$ (order-parameters of each electrode) across the junction, $I_c$ is the critical current. Usually $I_c$ is positive and the minimum of the Josephson energy $U = E_J(1 - \cos\phi)$, $E_J = \frac{I_c \Phi_0}{2\pi}$ is at $\phi = 0$. However, Bulaevskiĭ *et al.* [1] calculated the supercurrent through a JJ with ferromagnetic impurities in the tunnel barrier and predicted a negative supercurrent, $I_c < 0$. For $-I_c \sin(\phi) = 0$ the solution $\phi = 0$ is unstable and corresponds to the maximum energy $U = E_J(1 + \cos\phi)$, while $\phi = \pi$ is stable and corresponds to the ground state. Such JJs with $\phi = \pi$ in ground state are called $\pi$ junctions, in contrast to conventional 0 junctions with $\phi = 0$. In case of a $\pi$ Josephson junction the first Josephson relation is modified to $I_s(\phi) = -I_c \sin(\phi) = I_c \sin(\phi + \pi)$. In experiment the measured critical current in a single junction is always positive and is equal to $|I_c|$. It is not possible to distinguish 0 JJs from $\pi$ JJs from the current-voltage characteristic (IVC) of a single junction. The particular $I_c(T)$ [2] and $I_c(d_F)$ [3] dependencies for SFS/SIFS type junction are used to determine the $\pi$ coupled state. For low-transparency SIFS junctions the $I_c(d_F)$ dependence is given by

$$I_c(d_F) \propto \exp\left(\frac{-d_F}{\xi_{F1}}\right) \cos\left(\frac{d_F - d_F^{\rm dead}}{\xi_{F2}}\right), \qquad (1)$$

where $\xi_{F1}, \xi_{F2}$ are the decay and oscillation lengths of critical current and $d_F^{\rm dead}$ is the dead magnetic layer thickness [4]. For $\frac{1}{2}\xi_{F2}\pi < d_F - d_F^{\rm dead} < \frac{3}{2}\xi_{F2}\pi$ the coupling in ground state of JJs is shifted by $\pi$.

In a second work Bulaevskiĭ *et al.* [5] predicted the appearance of a *spontaneous* supercurrent at the boundary between a 0 and a $\pi$ coupled long JJ (LJJ). This supercurrent emerges in the absence of a driving bias current or an external field $H$, i.e. in the ground state. Depending on the length of the junction $L$ the supercurrent carries one half of the flux quantum, i.e. $\Phi_0/2$ (called

*semifluxon*), or less. Fig. 1(a) depicts the cross section of a symmetric 0–$\pi$ *long* JJ. The spontaneous supercurrent $j_s$ flows either clockwise or counterclockwise, creating the magnetic field of $\pm\Phi_0/2$. The current density jumps from maximum positive to maximum negative value at the 0–$\pi$ phase boundary. A theoretical analysis based on the perturbed sine-Gordon equation is given in Ref. [6]. Below we will first discuss the properties of the spontaneous supercurrent and, second, various systems having 0–$\pi$ phase boundaries.

*Spontaneous supercurrent* Kirtley *et al.* [7] calculated the free energy of 0–$\pi$ JJs for various lengths of the 0 and $\pi$ parts as a function of the normalized length $\ell = L/\lambda_J$ and the degree of asymmetry $\Delta = |j_c^\pi|L_\pi/|j_c^0|L_0$, where $j_c^0, j_c^\pi$ are the critical current densities and $L_0, L_\pi$ are the lengths of 0 and $\pi$ parts respectively, so that $L = L_0+L_\pi$. The state of a *symmetric* 0–$\pi$ junction ($\Delta = 1$) with spontaneous flux has lower energy than the states $\phi = 0$ or $\phi = \pi$ without flux. Symmetric 0–$\pi$ junctions have *always* some self-generated spontaneous flux, although its amplitude vanishes for $L \to 0$ as $\Phi \approx \Phi_0\ell^2/8\pi$. For example, a symmetric 0–$\pi$ JJ of the total length $L = \lambda_J$ has a spontaneous magnetic flux $\Phi \approx 0.04\Phi_0$ and a symmetric 0–$\pi$ JJ with $L = 8\lambda_J$ has a spontaneous flux of some $2-3\%$ below $\Phi_0/2$. Only in case of a infinitely long JJ we refer to the spontaneous flux as *semifluxons*, for shorter JJs it is named *fractional vortex*.

The supercurrent or magnetic flux can be directly detected by measuring $I_c(H)$ [7], by scanning SQUID (superconducting quantum interference device) microscopy (in the LJJ limit, see [8, 9]) or by LTSEM (low temperature scanning electron microscopy) [10].

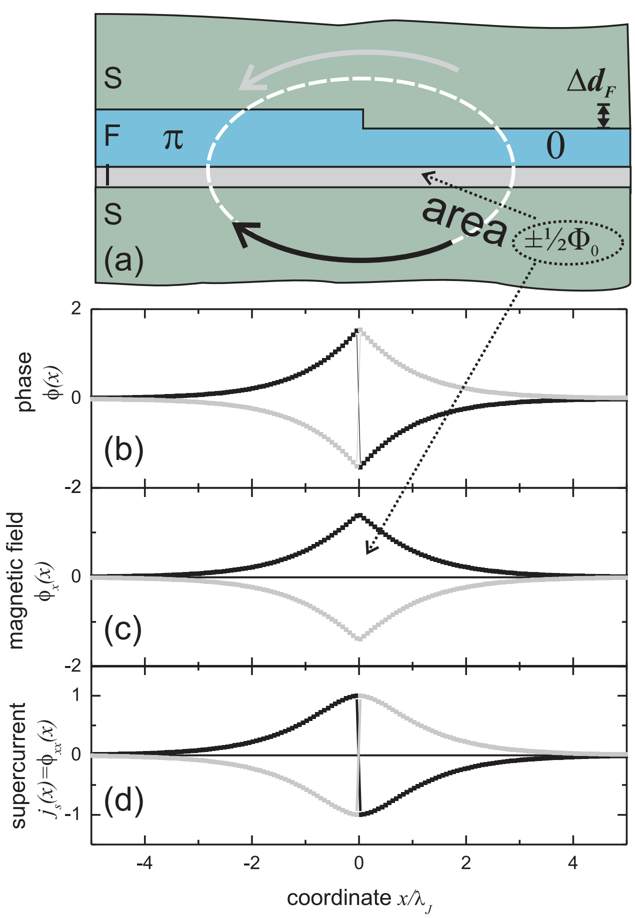


**Fig. 1** (a) Sketch of a 0–$\pi$ SIFS JJ with step-like thickness of F-layer and circulating supercurrent $j_s$ around 0–$\pi$ phase boundary. The junction length $L \gg \lambda_J$, therefore the spontaneous flux (area below magnetic field) is equal to half of a flux quantum $\Phi_0$ (semifluxon). (b)-(d) depicts the phase $\phi(x)$, magnetic field $\phi_x(x)$ and supercurrent $j_s(x) = \frac{I_c}{|I_c|}\sin\phi$ of the 0–$\pi$ junction.

*0–$\pi$ junctions technology* 0–$\pi$ Josephson junctions with a spontaneous flux in the ground state are realized with various technologies. The presence of fractional vortex has been demonstrated experimentally in *d*-wave superconductor based ramp zigzag junctions [9], in long Josephson 0–$\pi$ junctions fabricated using the conventional Nb/-Al-$Al_2O_3$/Nb technology with a pair of current injectors [11], in the so-called tricrystal grain-boundary LJJs [8, 12, 13] or in SFS/SIFS JJs [14, 15, 16] with *stepped* ferromagnetic barrier as in Fig. 1. In the latter systems the Josephson phase in the ground state is set to 0 or $\pi$ by choosing proper F-layer thicknesses $d_1$, $d_2$ for 0 and $\pi$ parts, i.e. the amplitude of the critical current densities $j_c^0$ and $j_c^\pi$ can be controlled to some degree. The advantages of this system are that it can be prepared in a multilayer geometry (allowing topological flexibility) and it can be easily combined with the well-developed Nb/Al-$Al_2O_3$/Nb technology.

The starting point for estimation of the ground state of a *stepped* JJ is studying the IVCs and $I_c(H)$ for the *planar* reference 0 and $\pi$ JJs. From this one can calculate important parameters such as the critical current densities $j_c^0$, $j_c^\pi$, the Josephson penetration depths $\lambda_J^0$, $\lambda_J^\pi$ and the ratio of asymmetry $\Delta$. For 0–$\pi$ junctions one needs 0 and $\pi$ coupling in *one* junction, setting high demands on the fabrication process. The ideal 0–$\pi$ JJ would have equal $|j_c^0| = |j_c^\pi|$ and a 0–$\pi$ phase boundary in its center to have a symmetric situation. Furthermore the junctions should be underdamped (SIFS structure) since low dissipation is necessary to study dynamics and eventually macroscopic quantum effects. The junctions should have a high $j_c$ (and hence small $\lambda_J \propto \sqrt{j_c}$) to reach the LJJ limit and to keep high $V_c = I_cR$ products, where $V_c$ is the characteristic voltage and $R$ the normal state resistance.

Previous experimental works on 0–$\pi$ JJs based on SFS technology [14, 15] gave no information about $j_c^0$ and $j_c^\pi$. Hence, the Josephson penetration depth $\lambda_J$ could not be calculated for these samples and the ratio of asymmetry $\Delta$ was unknown. The first intentionally made symmetric 0–$\pi$ tunnel JJ of SIFS type with a large $V_c$ was realized by the authors [16], making direct transport measure-

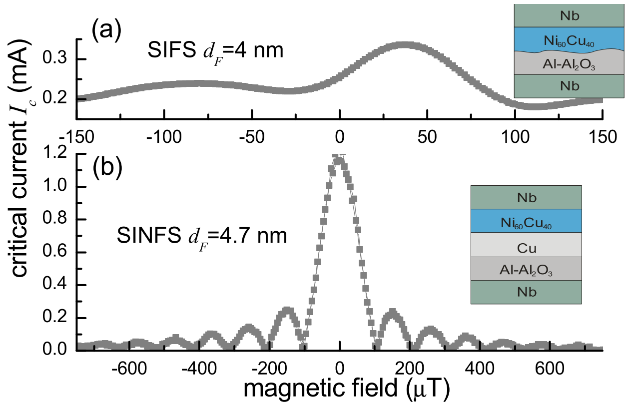


**Fig. 2** (Color online) $I_c(H)$ of (a) SIFS (4 nm NiCu) and (b) SINFS (Cu 2 nm, NiCu 4.7 nm) stacks. Oxygen pressure is 0.45 mbar for SIFS and 0.015 mbar for SINFS type.

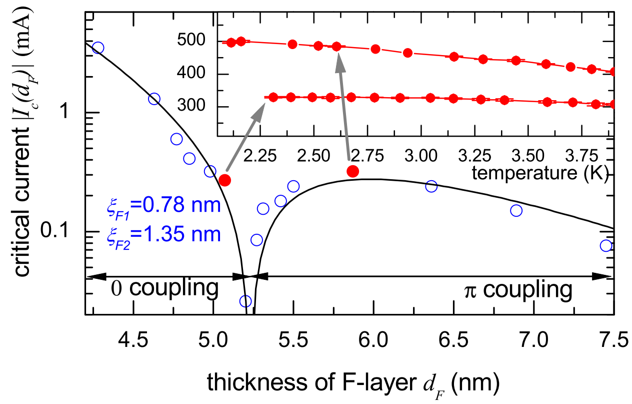


**Fig. 3** (Color online) $I_c(d_F)$ and $I_c(T)$ (inset) dependences of SIFS junctions at 4.2 K. Note the difference of the slope of $I_c(T)$ for 0 and $\pi$ coupled junction (inset).

ments of $I_c(H)$ and calculation of the ground state with spontaneous flux feasible.

Within this paper we *review* the physics of 0–$\pi$ coupled SIFS-type Josephson junctions and give an overview on our experimental results. Special focus is put on the fabrication of SIFS junctions having a planar or stepped-typed ferromagnetic layer (NiCu), the determination of ground state (0 or $\pi$ for planar JJs) and asymmetry of critical currents (stepped JJs). Finally we give an estimation of the spontaneous magnetic flux in the ferromagnetic 0–$\pi$ JJs.

## 2 Fabrication

The fabrication process for *planar* junctions is based on Nb/Al-$Al_2O_3$/NiCu/Nb stacks, deposited by dc magnetron sputtering [17]. Thermally oxidized 4-inch Si wafer served as substrate. First of all, a 120 nm thick Nb bottom electrode and a 5 nm thick Al layer were deposited. Second, the aluminium was oxidized for 30 min at room temperature in a separate chamber. Third, the ferromagnet (i.e. $Ni_{60}Cu_{40}$ alloy, $T_C = 225$ K) was deposited. To have many structures with different thicknesses in one fabrication run, we decided to deposit a *wedge*-shaped F-layer. For this the substrate and sputter target were shifted about half of the substrate diameter. This allowed the preparation of SIFS junctions with a gradient in F-layer thickness in order to minimize inevitable run-to-run variations. The sputtering rates for NiCu along the gradient were determined by thickness measurements on reference samples using a Dektak profiler. At the end a 40 nm Nb cap layer was deposited. The tunnel junctions were patterned using a three level optical photolithographic mask procedure and Ar ion-beam milling [18]. The insulation between top and bottom electrode is done by a self-aligned growth of $Nb_2O_5$ insulator by anodic oxidation of Nb after the ion-beam etching. The $Nb_2O_5$ exhibited a defect free insulation between the superconducting electrodes.

Topological and electrical measurements, see Ref. [17], indicated that the direct deposition of NiCu on the tunnel barrier (SIFS-stacks) led to an anomalous $I_c(H)$ dependence such as shown in Fig. 2(a), which is an indication for an inhomogeneous current transport. An additional 2 nm thin Cu layer between the $Al_2O_3$ tunnel barrier and the ferromagnetic NiCu (SINFS-stacks) brought considerable benefits, as it ensured a homogeneous current transport, see Fig. 2(b). In this way a high number of functioning devices with $j_c$ spreads less than 2% was obtained. The variation of the F-layer thickness over a length of one junction diameter is less than 0.02 nm. For simplification we refer in the following to SIFS stacks, although the actual multilayer is SINFS-type.
The patterning of *stepped* junctions was done after the complete deposition of the planar SIFS stack and before the definition of the junction mesa by argon-etching and $Nb_2O_5$ insulation. The detailed process is published in Ref. [19]. The junction was partly protected with photoresist to define the step location in the F-layer, followed by i) *selective reactive etching* of the Nb, ii) *ion-etching* of the NiCu by $\Delta d_F$ and iii) subsequent *in situ* deposition of Nb. To our knowledge, this was the first controlled patterning of 0–$\pi$ JJs based on a ferromagnetic interlayer.
The planar 0, $\pi$ reference junctions and the stepped 0–$\pi$ junctions were fabricated from a single trilayer.

## 3 SIFS junctions without step-like F-layer

All investigated junctions had an area of 10 000$\mu$m$^2$, but the length and width were different for different junctions. The length was comparable or shorter than the Josephson penetration depth $\lambda_J$. We investigated the thickness dependence of the critical current $I_c(d_F)$. To produce the $Al_2O_3$ barrier the Al layer was oxidized at 0.015 mbar yielding $j_c \approx 4.0$ kA/cm$^2$ for the reference superconductor-insulator-superconductor (SIS) JJs. Then SIFS stacks with wedge-like F-layer were fabricated in

another run. Taking the JJs of the same geometry ($100\times 100\ \mu\mathrm{m}^2$), but situated at different places on the wafer (i.e. different $d_F$) we have measured the nonmonotonic $I_c(d_F)$ dependence shown in Fig. 3. As a result the fitted parameters are $\xi_{F1} = 0.78$ nm, $\xi_{F2} = 1.35$ nm and $d_F^{\mathrm{dead}} \approx 3.09$ nm. The coupling changed from 0 to $\pi$ at the crossover thickness $d_F^{0\text{-}\pi} = \frac{\pi}{2}\xi_{F2} + d_F^{\mathrm{dead}} = 5.21$ nm [4].

The magnetic and spin-orbit scattering in the F-layer mixes the up and down spin states of electrons in the conduction bands. If the spin-flip scattering time $\tau_s$ is short $\hbar\tau_s^{-1} \gg k_B T_c$, like in NiCu alloys, the temperature dependence of scattering provides the dominant mechanism for the $I_c(T)$ dependence [20]. The oscillation period $\xi_{F2}$ becomes shorter for decreasing temperature, thus the whole $I_c(d_F)$ dependence is squeezed to thinner F-layer thicknesses. Hence, the temperature dependence of the critical current $I_c(T)$ is an interplay between an increasing component due to an increasing gap and a magnetic coupling dependent contribution which may de- or increase $I_c$. The $I_c(T)$ relations for two JJs (one 0, one $\pi$) are shown in the inset of Fig. 3. At $d_F = 5.11$ nm the JJ is 0 coupled, but one can relate the nearly constant $I_c$ below 3.5 K to the interplay between an increasing gap and a decreasing oscillation length $\xi_{F2}(T)$. The $d_F = 5.87$nm JJ is $\pi$ coupled and showed a linearly increasing $I_c$ with decreasing temperature.

## 4 SIFS junctions with step-like F-layer

Various structures on the wafer were placed within a narrow ribbon perpendicular to the gradient in the F-layer thickness and were replicated along this gradient. One ribbon contained reference JJs with the uniform F-layer thickness $d_1$ (uniformly etched) and $d_2$ (non-etched) and a JJ with a step $\Delta d_F$ in the F-layer thickness from $d_1$ to $d_2$. The lengths $L_{d_1}$ and $L_{d_2}$ are both equal to 167 $\mu$m. The lithographic accuracy is of the order of 1 $\mu$m. A set of structures with difference in $d_F$ between neighboring ribbons of 0.05 nm was obtained. Comparing the critical currents $I_c$ of non-etched JJs (dots), see Fig. 4 with the experimental $I_c(d_F)$ data for the etched samples (stars) we estimate the etched-away F-layer thickness as $\Delta d_F \approx 0.3$ nm. The stars in Fig. 4 are shown already shifted by this amount. Now we choose the set of junctions which have the thickness $d_2$ and critical current $I_c(d_2) < 0$ ($\pi$ junction) before etching and have the thickness $d_1 = d_2 - \Delta d_F$ and critical current $I_c(d_1) \approx -I_c(d_2)$ (0 junction) after etching. One option is to choose the junction set denoted by closed circles around the data points in Fig. 4, i.e. $d_1 = 5.05$ nm and $d_2 = 5.33$ nm.

The $I$-$V$ characteristics and the magnetic field dependence of the critical current $I_c(H)$ was measured for all three junctions: 0 JJ with $d_F = d_1$, $\pi$ JJ with $d_F = d_2$ and 0–$\pi$ JJs with stepped F-layer ($d_1$ and $d_2$ in each half). The magnetic diffraction pattern $I_c(H)$ of the 0–$\pi$ JJ and the 0 and $\pi$ reference JJs are plotted in Fig. 5. The magnetic field $H$ was applied in-plane of the sample and parallel to the step in the F-layer. Due to a small net magnetization of the F-layers the $I_c(H)$ of references junctions were slightly shifted along the $H$ axis. Nevertheless, both had the same oscillation period $\mu_0 H_{c1} \approx 36\ \mu$T. At $T \approx 4.0$ K the 0–$\pi$ JJs was slightly asymmetric with $I_c^0 \approx 208\ \mu$A and $I_c^\pi \approx 171\ \mu$A (data of reference JJs). To achieve a more symmetric configuration, the bath temperature was reduced, because a decrease in temperature should increase $I_c^\pi = I_c(d_2)$ more than $I_c^0 = I_c(d_1)$, like for the 0 and $\pi$ samples in the inset of Fig. 3. As a result, both $I_c^0(T)$ and $I_c^\pi(T)$ were increasing when decreasing the temperature, but with different rates. At $T \approx 2.65$ K the critical currents $I_c^0$ and $I_c^\pi$ became approximately equal, see Fig. 5. The magnetic field dependence of the planar reference junctions $I_c^0(H)$ and $I_c^\pi(H)$ look like perfect Fraunhofer patterns. One can see that the $I_c^0(H)$ and $I_c^\pi(H)$ measurements almost coincide, having the form of a symmetric Fraunhofer pattern with the critical currents $I_c^0 \approx 220\ \mu$A, $I_c^\pi \approx 217\ \mu$A and the same oscillation period. The stepped 0–$\pi$ junction had a magnetic field dependence $I_c^{0\text{-}\pi}(H)$ with a clear minimum near zero field and almost no asymmetry. The critical currents at the left and right maxima (146 $\mu$A and 141 $\mu$A) differ by less than 4 %, i.e. the 0–$\pi$ junction is symmetric, and its ground state in absence of a driving bias or magnetic field ($I = H = 0$) can be calculated [16]. Our symmetric 0–$\pi$ LJJ had an normalized length of $\ell = 1.3$, with a spontaneous flux in the ground state of

$$\pm\Phi \approx \Phi_0 \ell^2/8\pi \approx 0.067\cdot\Phi_0,$$

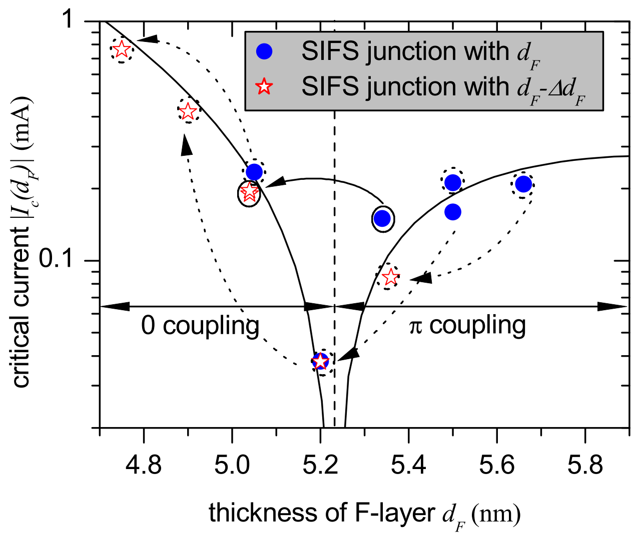


**Fig. 4** (Color online) Critical current $I_c$ of the uniformly etched (star) and non-etched (dot) SIFS junctions versus the F-layer thickness before etching $d_F$. The fit of the experimental data for non-etched samples using Eq.(1) is shown by the continuous line. The JJs were oxidized at 0.015 mbar.

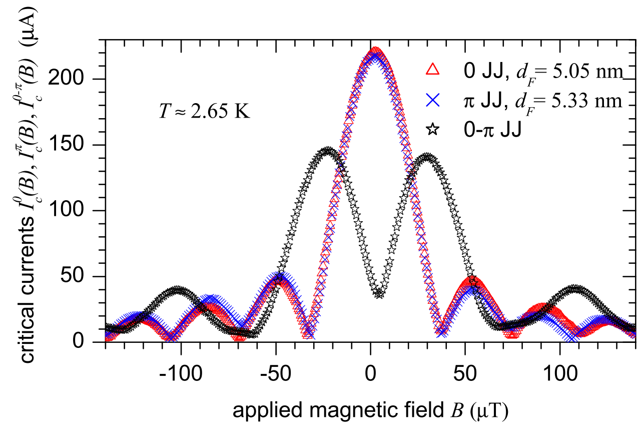


**Fig. 5** (Color online) $I_c(H)$ of 0–$\pi$ JJ (open triangles) with $H$ applied parallel to short axis, overlayed with the non-etched (dot) and etched (stars) reference SIFS junction measurements. At $T \approx 2.65$ K the 0–$\pi$ JJ becomes symmetric. The junction dimensions are $330 \times 30$ $\mu$m$^2$.

being equal to 13% of $\Phi_0/2$. A detailed calculation taking several deviations from the ideal short JJ model into account can be found elsewhere [21].

## 5 Summary

The concept and realization of 0-$\pi$ junction based on SIFS stacks has been presented. The realization of $\pi$ coupling in SIFS junctions and the precise combination of 0 and $\pi$ coupled parts in a single junction has been shown. The coupling of the ferromagnetic Josephson tunnel junctions was investigated by means of transport measurements. The emergence of a spontaneous flux, which was calculated as 13% of half a flux quantum $\Phi_0/2$, was observed in the magnetic field dependence of the current-voltage characteristics of the 0–$\pi$ JJ.
As an outlook, the ferromagnetic 0–$\pi$ Josephson junctions allow to study the physics of fractional vortices with a good temperature control of the symmetry between 0 and $\pi$ parts. We note that symmetry is only needed for JJ lengths $L \lesssim \lambda_J$. For longer JJs the semifluxon appears even in rather asymmetric JJs, and $T$ can be varied in a wide range affecting the semifluxon properties only weakly. The presented SIFS technology allows us to construct 0, $\pi$ and 0–$\pi$ JJs with comparable $j_c^0$ and $j_c^\pi$ in a single fabrication run. Such JJs may be used to construct classical and quantum devices such as oscillators, memory cells, $\pi$ flux qubits [22, 23] or semifluxon based qubits [24].

## Acknowledgment

This work was suportted by Heraeus Foundation and the Deutsche Forschungsgemeinschaft (projects SFB/TR 21).

## References

1. L. Bulaevskiĭ, V. Kuziĭ and A. Sobyanin, JETP Lett. **25**, 7 (1977).
2. A. V. Veretennikov, V. V. Ryazanov, V. A. Oboznov, A Yu. Rusanov, V. A. Larkin and J. Aarts, Physica B **284**, 495 (2000).
3. T. Kontos, M. Aprili, J. Lesueur and X. Grison, Phys. Rev. Lett. **89**, 137007 (2002).
4. M. Weides, M. Kemmler, E. Goldobin, D. Koelle, R. Kleiner, H. Kohlstedt and A. Buzdin, Appl. Phys. Lett. **89**, 122511 (2006).
5. L. N. Bulaevskiĭ, V. V. Kuziĭ and A. A. Sobyanin, Solid State Commun. **25**, 1053 (1978).
6. E. Goldobin, D. Koelle and R. Kleiner, Phys. Rev. B **66**, 100508 (2002).
7. J. R. Kirtley, K. A. Moler and D. J. Scalapino, Phys. Rev. B **56**, 886 (1997).
8. J. R. Kirtley, C. C. Tsuei, M. Rupp, J. Z. Sun, L. S. Yu-Jahnes, A. Gupta, M. B. Ketchen, K. A. Moler and M. Bhushan, Phys. Rev. Lett. **76**, 1336 (1996).
9. H. Hilgenkamp, Ariando, H. J. H. Smilde, D. H. A. Blank, G. Rijnders, H. Rogalla, J. R. Kirtley and C. C. Tsuei, Nature (London) **422**, 50 (2003).
10. R. Gross and D. Koelle, Rep. Prog. Phys. **57**, 651 (1994).
11. E. Goldobin, A. Sterck, T. Gaber, D. Koelle and R. Kleiner, Phys. Rev. Lett. **92**, 057005 (2004).
12. J. R. Kirtley, C. C. Tsuei and K. A. Moler, Science **285**, 1373 (1999).
13. A. Sugimoto, T. Yamaguchi and I. Iguchi, Physica C **367**, 28 (2002).
14. S. M. Frolov, D. J. Van Harlingen, V. V. Bolginov, V. A. Oboznov and V. V. Ryazanov, Phys. Rev. B **74**, 020503 (2006).
15. M. L. Della Rocca, M. Aprili, T. Kontos, A. Gomez and P. Spatkis, Phys. Rev. Lett. **94**, 197003 (2005).
16. M. Weides, M. Kemmler, H. Kohlstedt, R. Waser, D. Koelle, R. Kleiner and E. Goldobin, Phys. Rev. Lett. **97**, 247001 (2006).
17. M. Weides, K. Tillmann and H. Kohlstedt, Physica C **437-438**, 349 (2006).
18. M. Gurvitch, M. A. Washington, H. A. Huggins and J. M. Rowell, IEEE Trans. Magn. **19**, 791 (1983).
19. M. Weides, C. Schindler and H. Kohlstedt, J. Appl. Phys. **101**, 063902 (2007).
20. V. A. Oboznov, V. V. Bol'ginov, A. K. Feofanov, V. V. Ryazanov and A. I. Buzdin, Phys. Rev. Lett. **96**, 197003 (2006).
21. M. Weides, H. Kohlstedt, J. Pfeiffer, M. Kemmler, D. Koelle, R. Kleiner and E. Goldobin, in preparation.
22. T. Yamashita, K. Tanikawa, S. Takahashi and S. Maekawa, Phys. Rev. Lett. **95**, 097001 (2005).
23. T. Yamashita, S. Takahashi and S. Maekawa, Appl. Phys. Lett. **88**, 132501 (2006).

24. E. Goldobin, K. Vogel, O. Crasser, R. Walser, W. P. Schleich, D. Koelle and R. Kleiner, Phys. Rev. B **72**, 54527 (2005).